

## CHAPTER 3

---

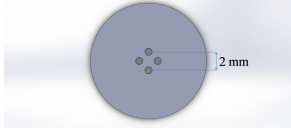




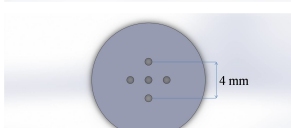
### Characterization of performance of multihole nozzle in cryospray and optimisation of its spray parameter

---

The present study is an attempt to resolve the challenges associated with the current practice of cryospray regarding the treatment of larger lesions, through the improvement in conventional technique of spraying liquid nitrogen on cancerous lesion. A multihole nozzle (MHN) with 5 holes is fabricated to demarcate the variation in outcome when cryogen is sprayed through customised MHN instead of conventional SHN. A special emphasis is placed on reducing the number of sitting required for the completion of treatment and increasing the feasibility of cryospray process for larger lesions. Commercial SHN having a hole diameter of 0.8 mm is selected to compare results with the customised MHN having 5 holes of 0.8 mm diameter (4 holes are arranged in a circle of radius 2 mm around the central hole). A single freeze-thaw cycle is carried out to spray liquid nitrogen on tissue mimicking gel.

In order to demarcate the impact of nozzle geometry on cryoablation, two sets of MHNs are fabricated. First set comprises of three MHNs each having 5 holes; one at the centre and 4 inscribed in a circular pattern around it. The exit diameter of commercial SHNs (provided by companies like SMT Praha and Brymill) varies in the range of 0.4 mm–0.8 mm. It is noticed that 0.8 mm hole diameter provides finely atomised spray [4, 5]. Moreover, decreasing the nozzle size decreases the spray zone which results in less cooling effect. Therefore, 0.8 mm diameter is selected as the nozzle diameter to present a comparative study between the commercial and customized nozzles. Distance between

Table 3.1: Nozzle Geometry

Schematic Diagram of MHN	Nomenclature
	4A
	4B
	4C
	5A
	5B
	5C

the centres of outer hole and the central hole is termed as margin between the holes. This margin is taken as 1 mm, 1.5 mm and 2 mm to complete the first set of MHN. In the second set, three MHNs with 4 holes inscribed in a circular pattern are manufactured while removing the central hole. The margins are selected in such a way that individual jets should not interact with each other to form a single jet during their flight from nozzle exit to the gel surface. The remaining parameters are kept same as in the first set of MHNs. Details of nozzle geometry is provided in Table 3.1. All MHNs are flat faced nozzle.

### 3.1 Materials and Method

Cryogen (liquid nitrogen) is sprayed using cryogun (CS-1) procured from SMT Praha, Czech Republic. The operating pressure of the cryogun is 70 kPa (gauge). Scales are mounted on different locations to measure the extent of radial and axial ice balls. Agarose powder (Low EEO, HIMEDIA Chemicals, CAS: 9012-36-6, catalogue no. MB002-500G) is used for mak-

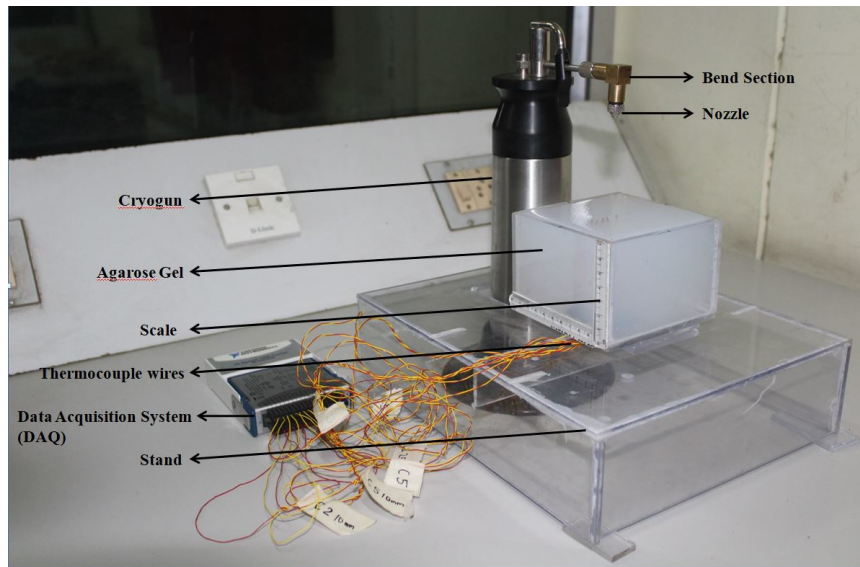


Figure 3.1: Experimental Setup

ing the tissue mimicking gel. Acrylic sheet is used to make the cuboid container for storing the gel. A K-type thermocouple with an accuracy of  $\pm 2$   $^{\circ}\text{C}$  is used to measure temperature at the discrete locations. Data acquisition system (National Instruments, USB 9213, US) is used to record temperature with respect to time. FLIR E 75 thermal imaging camera with an accuracy of  $\pm 2$   $^{\circ}\text{C}$  is used to capture the thermal images at various time steps. These images provide temperature profile on the surface of gel.

Fig. 3.1 shows the experimental setup used for the study. Tissue mimicking gel is prepared through dissolving 5.4 g of agarose powder in 900 ml of distilled water and heating it in a microwave oven (900W) for 9 min. The heated gel is cooled to the ambient temperature, and then it is poured into a cuboid container for solidification. Solidification of gel is carried out in ambient atmosphere to promote natural thawing for 8 h. Quantity of agarose powder and water is selected in such a way that 0.6 w/v concentration can be ensured in gel because it resembles the property of dermis [96]. The cuboid container has a dimension of  $100 \times 100 \times 70$   $\text{mm}^3$ . Continuous spray technique is used to spray liquid nitrogen on the gel for 120 s followed by a thawing duration of 130 s. The spray duration is taken as 120 s to demonstrate the extent of cryoablation as time proceeds. It can be varied depending on the lesion dimension and orientation. To record the temperature, five thermocouples are placed at a distance of 2 mm from the surface of the gel. Since the case is symmetric, all the 5 thermocouples are placed on the left side of the centre of spray. Distance of the thermocouples with respect to the centre of spray (CS) is taken as 0 mm, 10 mm, 15 mm, 20 mm and 25 mm. The average thickness of dermis, i.e. 1.8–2 mm [34, 142, 169], is the reason to mount the thermocouples at that location. In addition to these

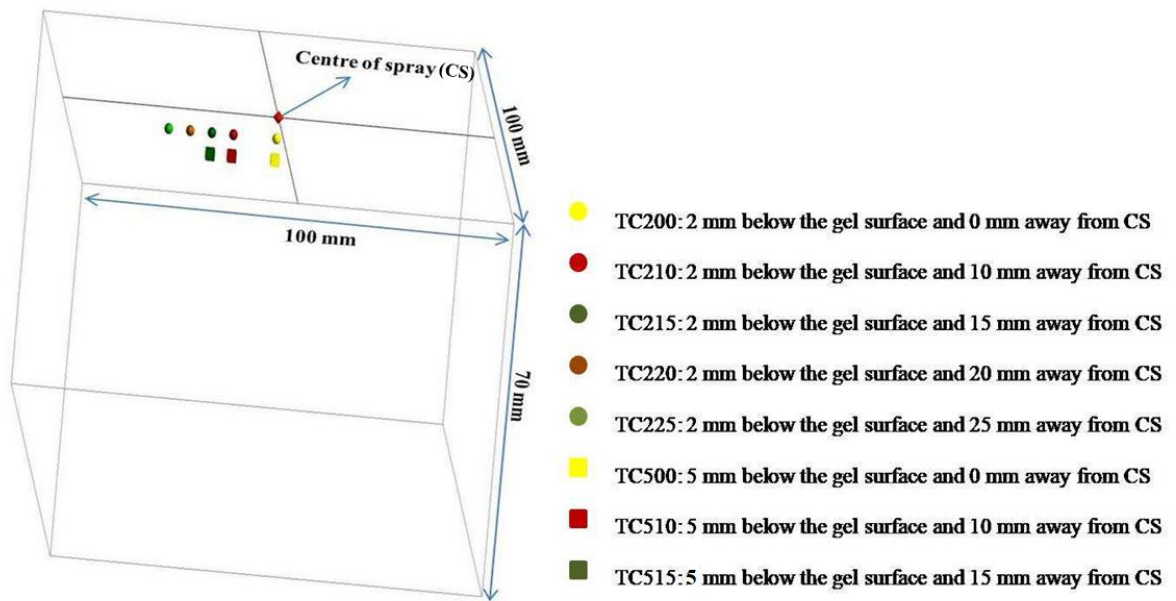


Figure 3.2: Positions of thermocouple

thermocouples, three thermocouples are also positioned at 5 mm below the surface of the gel. All the three thermocouples are placed on the left side of the CS. The distance is also kept same as 0 mm, 10 mm, and 15 mm respectively. Nomenclature of thermocouples on the basis of their orientation is depicted in Fig. 3.2. The spraying distance is kept constant at 18 mm throughout the study. As for the nozzles used in current practice, the suggested spraying distance is 15–20 mm [170].

## 3.2 Results and discussions

The temperature variation with respect to time is measured in axial and radial directions experimentally to study the impact of nozzle geometry on cryoablation. Axial temperature distribution is quantified through the placement of thermocouples at the discrete locations. Thermal imaging camera is employed to quantify the temperature distribution in radial direction. Propagation of freezing front in axial direction is estimated while taking images through Canon DSLR camera. Further, data is extracted through images using Labview software.

### 3.2.1 Uncertainty Analysis

To ensure repeatability in results, each experiment is performed several times. Mean and standard deviations are calculated through data sets and values are plotted against mean. There are two sources of uncertainty in the temperature measurements: (i) stochastic uncertainty ( $\delta_{st}$ ) and (ii) systematic uncertainty ( $\delta_{sys}$ ). Stochastic uncertainty is calculated using student's t-test in the following manner [75]:

$$\delta_{st} = \frac{\tau s}{\sqrt{n}}$$

Where,  $\delta_{st}$  is the uncertainty in the temperature measurement,  $n$  is the number of measurements,  $\tau$  is the Student's t-statistic for the probability less than 0.025 based on  $(n-1)$  degrees of freedom, and  $s$  is the standard deviation of the measurement. Thermocouple is immersed in liquid nitrogen for 1 minute and its temperature is found to be  $-194\text{ }^{\circ}\text{C}$ . Therefore, the error in temperature measurement due to thermocouple is  $2\text{ }^{\circ}\text{C}$  [132]. It is accounted as systematic uncertainty ( $\delta_{st}$ ) [158, 166].

$$\delta_{overall} = \sqrt{(\delta_{st})^2 + (\delta_{sys})^2}$$

The overall uncertainty ( $\delta_{overall}$ ) is found through the method mentioned in Bevington and Robinson [18].

Positioning error is caused by possible dislocation of the TC junction from the mean position. Before conducting the experiment, location of each thermocouple is estimated and found to vary in the range of  $\pm 0.5\text{ mm}$  from the mean position. All experiments were conducted in between 7-8 pm IST. Fig. 3.3 represents temperature history of thermocouples mounted at TC200 and TC500 location. Mean and standard deviation is calculated through data sets and values are plotted along mean. The error bars shown in fig. 3.3 are at 95% confidence interval. The temperature measurement data has an overall uncertainty of  $\pm 15\text{ }^{\circ}\text{C}$ . Several cases reported in literature [37, 75, 139] suggest uncertainty in temperature measurement from  $\pm 10\text{ }^{\circ}\text{C}$  to  $\pm 15\text{ }^{\circ}\text{C}$  depending upon the nature of study. It is acceptable in this case, because [37, 75, 139] are related to cryotherapy in which cryogen does not come in direct contact with the atmosphere while the present case deals with cryospray, which is an open spray technique. Maximum uncertainty is recorded in

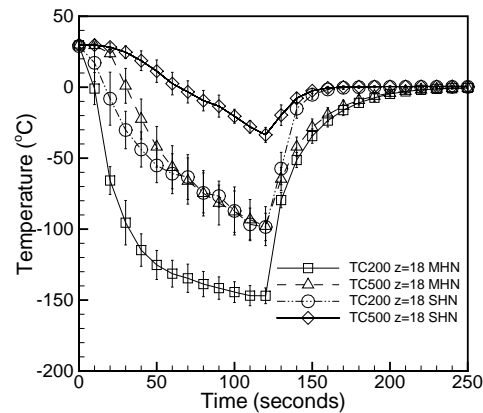


Figure 3.3: Transient temperature curves of thermocouples placed at 2 mm and 5 mm below the gel surface and 0 mm away from CS with 95% confidence interval for  $z=18$  mm (MHN: Multihole nozzle, SHN: Singlehole nozzle,  $z$ : Spraying distance)

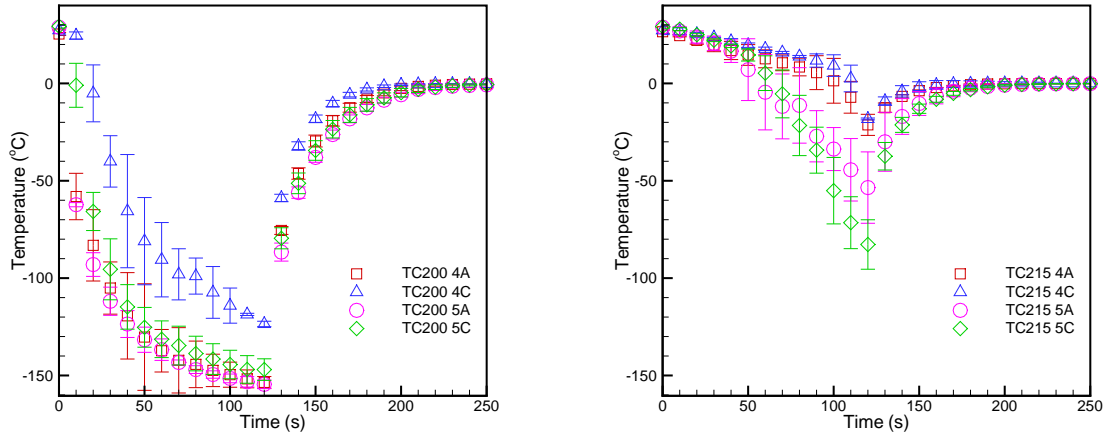
the initial phase of spray because liquid nitrogen gushes out of the pressurised tank with huge temperature difference compared to the surrounding which requires some time to stabilise the flow.

Similarly, temperature history for MHNs 4A, 4C, 5A, and 5C at TC200 and TC215 locations is shown in fig. 3.4 for reference. The figure clearly indicates that the maximum uncertainty of temperature is below  $\pm 15^{\circ}\text{C}$ . This figure also reveals the significant difference in temperature variation caused by the number of holes and margin among the holes.

### 3.2.2 Validation of thermal images

FLIR Tools software is used to extract data from thermal images. During data extraction from thermal images it is observed that minimum temperature recorded by temperature contours is  $-40^{\circ}\text{C}$ . However, as per the specifications of FLIR E75 camera it works in the temperature range of  $-20^{\circ}\text{C}$  to  $-120^{\circ}\text{C}$ . So an experiment is designed to verify this variation in temperature range of IR camera. Cryogen is sprayed through MHN 5C while keeping the rest parameters same. Three thermocouples are mounted on the surface of the gel; the radial distance of thermocouples from CS is taken as 10 mm, 15 mm and 20 mm. Experiment is performed and images are captured at every 10 s during 120 s of spray. Data extracted through thermal images and thermocouple is listed in table 3.2.

It can be noticed that the thermocouple mounted at 10 mm from CS requires 50-60 s to reach temperature below  $-40^{\circ}\text{C}$  while the thermocouple mounted at 15 mm from CS



(a) 2 mm below the gel surface and 0 mm away from CS      (b) 2 mm below the gel surface and 15 mm away from CS

Figure 3.4: Transient temperature curves of thermocouples placed at 2 mm below the gel surface with 95% confidence interval for nozzle 4A, 4C, 5A, and 5C

Table 3.2: Verification of data generated through FLIR Camera

Time(s)	Data extracted through			Data recorded in DAQ		
	FLIR Tools software( $^{\circ}$ C)			through thermocouples( $^{\circ}$ C)		
	10 mm from CS	15 mm from CS	20 mm from CS	10 mm from CS	15 mm from CS	20 mm from CS
0	31	31	31	31	31	31
10	-1	9	17	25	26	24
20	-10	8	19	18	21	21
30	-34	-2	11	13	17	17
40	-35	-2	12	2	13	13
50	-38	-12	1	-18	9	9
60	-40	-17	0	-65	5	6
70	-40	-21	-2	-114	-29	1
80	-40	-40	-3	-129	-74	0
90	-40	-40	-3	-122	-56	-2
100	-40	-40	-5	-129	-67	-6
110	-40	-40	-13	-135	-77	-11
120	-40	-40	-33	-141	-94	-18

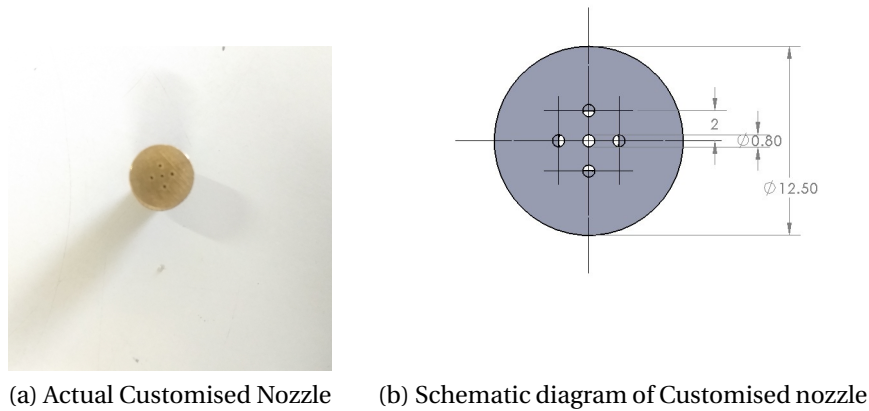


Figure 3.5: Customised Nozzle

requires 70-80 s. Whereas, for thermocouple positioned at 20 mm from CS, temperature below  $-40^{\circ}\text{C}$  is not achieved. Now, if data generated through FLIR Tools software is analysed acknowledging the fact that minimum temperature that it can record is  $-40^{\circ}\text{C}$ , it can be seen that  $-40^{\circ}\text{C}$  is shown after 50-60 s and 70-80 s after the start of spray for the position of 10 mm and 15 mm from the CS respectively. It can be interpreted through these observations that time range in which temperature below  $-40^{\circ}\text{C}$  is encountered is same for both the data sets. It also strengthens the fact that data shown through thermal image processing in terms of minimum temperature is correct and authentic. Although issues like obstruction created in propagation of freezing front when thermocouples are mounted in upside down direction cannot be overruled. Temperature recorded through thermocouple is higher as compared to temperature produced through FLIR Tools software at a particular instant. Reason for this variation is the insertion of thermocouple beads inside the gel. As FLIR data is representing temperature exactly on the gel surface while thermocouples are showing temperature slightly below the surface.

### 3.2.3 Comparison of cryoablation between SHN and MHN

This study provides a comparative analysis of cryoablation when cryogen is sprayed through SHN and MHN, two types of nozzle are selected: (i) commercial SHN procured from SMT Praha, Czech Republic with outlet hole diameter of 0.8 mm (refer Fig. 3.6a and 3.6b) and (ii) customised MHN consisting of 5 holes of diameter 0.8 mm (refer Fig. 3.5a and 3.5b). Commercial nozzle has a conical shape while customised nozzle has a flat face. Flat face geometry is preferred to ensure constant spraying distance between the tissue

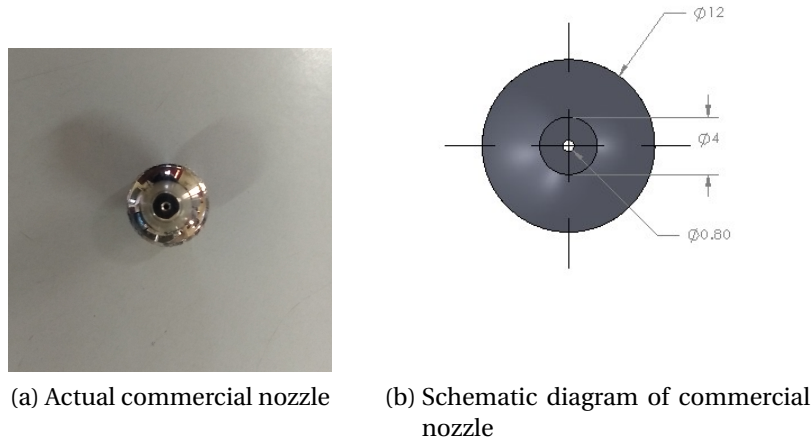
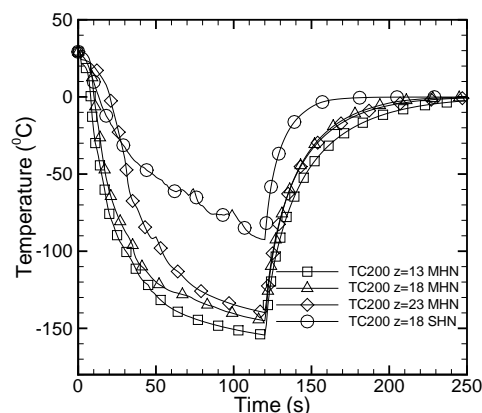


Figure 3.6: Commercial nozzle

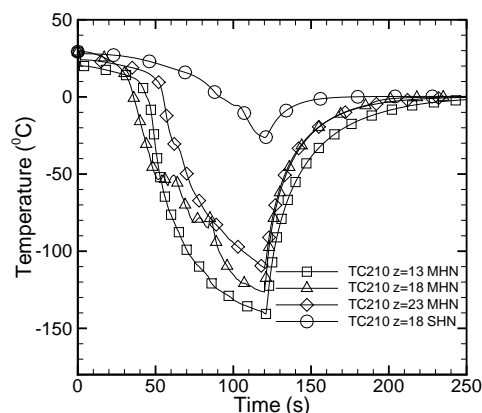
phantom and each individual jet of MHN. Three spraying distances (i.e.,  $z = 13$  mm,  $z = 18$  mm and  $z = 23$  mm) are selected to spray the cryogen from MHN.

### 3.2.3.1 Axial temperature distribution

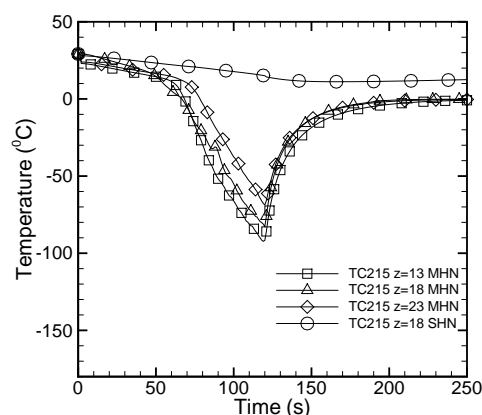
Total 8 thermocouples are mounted in the experimental setup to record temperature distribution. Figs. 3.7a and 3.8a show temperature variation among the thermocouples mounted at 2 mm and 5 mm below the CS. The minimum temperature recorded by the thermocouple, mounted at a location of 2 mm below CS, after 120 s spray is  $-145$  °C and  $-92$  °C for MHN and SHN respectively when  $z = 18$  mm. Difference in temperature drop between SHN and MHN is approximately  $50$  °C. This difference remains same for the thermocouple mounted at 5 mm below the centre of spray, as the minimum temperature after 120 s of spray is  $-90$  °C and  $-33$  °C for MHN and SHN respectively. Furthermore, for thermocouples placed at TC210, TC215, TC220 and TC225 locations, the lowest temperature recorded after 120 s of spray is found to be  $-126$  °C,  $-82$  °C,  $-3$  °C,  $18$  °C and  $-26$  °C,  $-15$  °C,  $17$  °C,  $22$  °C for MHN and SHN respectively. Similarly, the lowest temperature found at TC510 and TC515 locations is  $-70$  °C,  $-41$  °C and  $8$  °C,  $22$  °C after 120 s of spray for MHN and SHN respectively. The temperature drop in MHN is higher because of higher mass flow rate. MHN under consideration has 5 holes and the distance of adjacent holes from the central hole is 2 mm. Since holes are quite close to each other, it reduces the interaction of individual jet from the ambient air. This reduces the rate of evaporation of cryogen during its flight from nozzle outlet to the phantom surface, which ultimately increases the extent of coldness and helps in achieving the low temperature.



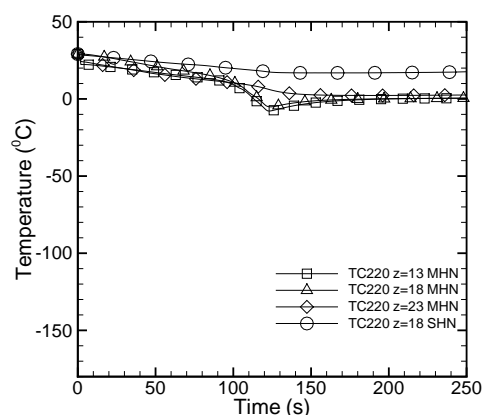
(a) 2 mm below gel surface and 0 mm away from centre of spray (TC200 location)



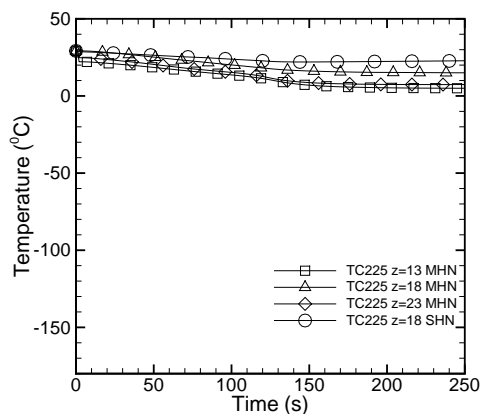
(b) 2 mm below gel surface and 10 mm away from centre of spray (TC210 location)



(c) 2 mm below gel surface and 15 mm away from centre of spray (TC215 location)

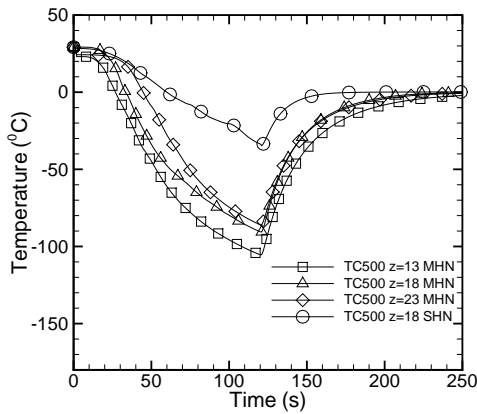


(d) 2 mm below gel surface and 20 mm away from centre of spray (TC220 location)

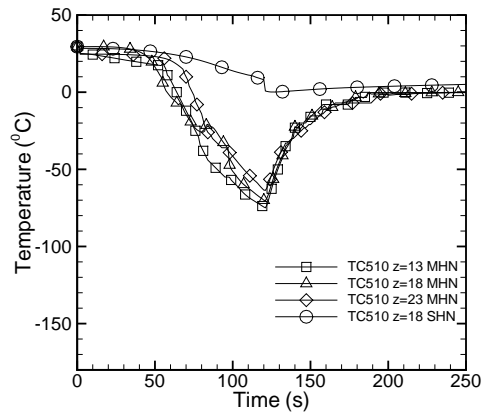


(e) 2 mm below gel surface and 25 mm away from centre of spray (TC225 location)

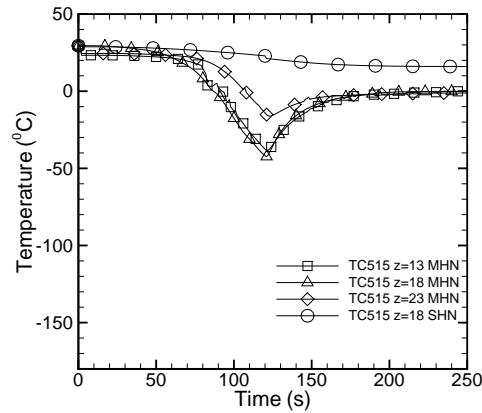
Figure 3.7: Transient temperature curves of thermocouples placed at 2 mm below the gel surface and at different radial locations (MHN: Multihole nozzle, SHN: Single-hole nozzle z: spraying distance)



(a) 5 mm below gel surface and 0 mm away from centre of spray (TC500 location)



(b) 5 mm below gel surface and 10 mm away from centre of spray (TC510 location)



(c) 5 mm below gel surface and 15 mm away from centre of spray (TC515 location)

Figure 3.8: Transient temperature curves of thermocouples placed at 5 mm below the gel surface and at different radial locations (MHN: Multihole nozzle, SHN: Single-hole nozzle z: spraying distance)

Another important factor is the extent of necrotic zone. From fig. 3.7 and fig. 3.8, it can be inferred that the lethal temperature (temperature  $< -40^{\circ}\text{C}$ ) is easily achieved up to 15 mm from CS and 2 mm below the surface using MHN. Whereas, the lethal temperature is not achieved even for a thermocouple placed at 10 mm away from CS and at a depth of 2 mm using SHN. For the thermocouples placed at 5 mm below the surface, at a distance of 0 mm, 10 mm and 15 mm away from the centre of spray, temperature below lethal temperature is not achieved in SHN while for MHN it can be achieved up to 15 mm. It can be inferred from this observation that MHN provides almost twice increment in the necrotic zone than SHN for the same spraying distance, i.e.  $z = 18$  mm.

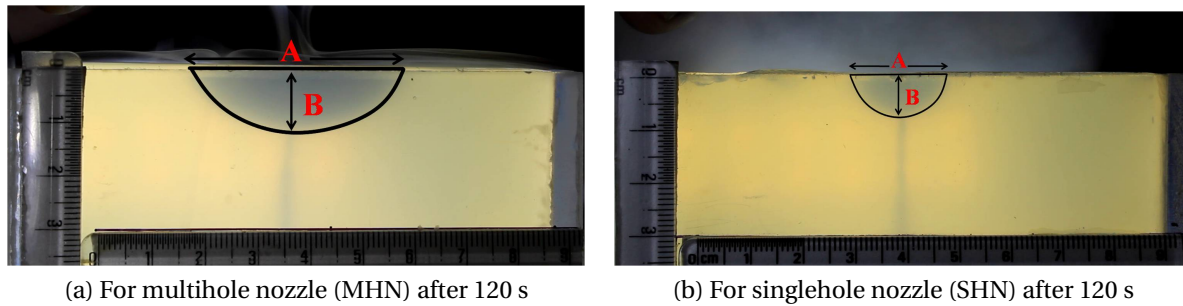
In order to optimise the spraying distance, three spraying distances are selected for the study when cryogen is sprayed through MHN. On reducing the spraying distance from 18 mm to 13 mm, a decrement in minimum temperature is recorded, while on increasing the spraying distance from 18 mm to 23 mm an increment in minimum temperature is recorded. Reason for such variation is the increase in the rate of evaporation of cryogen with increment in spraying distance, which is quite obvious. The overall variation in temperature at each location is found to be in the range of  $\pm 20^{\circ}\text{C}$  when spraying distance is varied to  $\pm 5$  mm from its position of 18 mm.

Table 3.3 lists the CR experienced by various thermocouples. CR is estimated for various thermocouples through the method mentioned in [75]. The mechanism of cell destruction depends on CR and the amount of cell destruction depends on both CR and ET [37, 41, 138]. If lethal temperature is reached, cell death is certain but there are areas where lethal temperature has not crossed but certainty of cell death can be assured if that area falls under the specific range of CR and its corresponding ET [138]. Data mentioned in the table 3.3 clearly reflects that MHN is capable enough to provide more cellular destruction as compared to SHN. The spread of necrotic zone is approximately 15 mm from the CS with a penetration depth of 5 mm while in case of SHN, it is restricted in the vicinity of CS only. For the intracellular cell destruction, CR of  $50^{\circ}\text{C}/\text{min}$  to  $200^{\circ}\text{C}/\text{min}$  is required for complete necrosis of tissue [164]. For the same spraying distance of  $z = 18$  mm, intracellular ice formation is recorded up to TC210 location in MHN while for SHN, it is totally absent. In the case of SHN, CR is lower than the required CR for intracellular cell destruction. But, combined effect of CR and ET causes extracellular cell destruction, possible up to 10 mm radius from CS at an axial depth of 2 mm. At TC215 location, cell destruction is possible due to the combined effect of intracellular and extracellular ice formation for MHN whereas for SHN, freezing is not observed at this location. Moreover, cyoablation can be assured at TC500, TC510 and TC515 in case of MHN while for SHN only TC500 provides cryoablation through the combination of intracellular and extracellular ice formation.

Table 3.3: Cooling Rate ( $^{\circ}\text{C}/\text{min}$ ) for various thermocouples for a spraying distance of ( $z$ ) = 18 mm

Position of thermocouple	Multihole nozzle (MHN)	Singlehole nozzle (SHN)
TC200	72	45
TC210	62	10
TC215	41	-
TC220	1	-
TC225	-	-
TC500	45	16
TC510	35	-
TC515	20	-

“-” freezing of gel is not observed

Figure 3.9: Propagation of ice front for spraying distance ( $z$ )=18 mm

### 3.2.3.2 Movement of axial ice front

Fig. 3.9 represents ice ball formed after 120 s of spray. Due to the translucent nature of agarose gel LED lights are placed behind the container to capture the images. Scales are mounted on the container to measure the dimension of the ice ball. There are studies related to the spray of cryogen through SHN in literature [97, 168, 195] and each one of them tried to quantify the relation between lateral spread and penetration depth according to their experimental conditions. But, this study is a maiden attempt to demarcate how freezing front propagates when MHN is applied instead of SHN to spray cryogen from the same spraying distance of 18 mm. For SHN, similar trend of ice ball propagation is observed as reported by Kumari et al. [97]. Penetration depth of ice ball is recorded as  $B = 8$  mm in axial direction while it is found to be  $A = 24$  mm in lateral direction. For MHN, ice ball formed has a penetration depth of  $B = 12$  mm in axial direction and  $A = 40$  mm in lateral direction. However, it is interesting to note that even after having multiple holes, formation of multiple freezing fronts is not observed for MHN. Multiple freezing front refers to a case where each jet has its own ice ball formation and it propagates independently. This

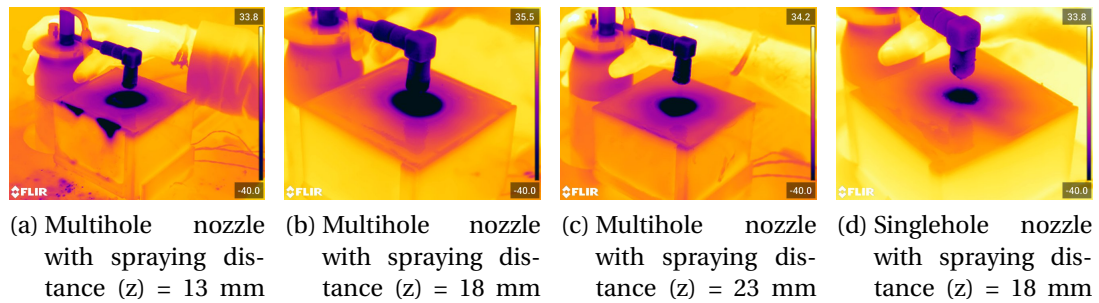


Figure 3.10: Thermal Images after 120 s of spray

is further validated through images captured from IR camera which is taken to estimate temperature distribution on the gel surface. The image taken after 10 s of spray does not depict any individual dark spot of minimum temperature featured around the individual jet. So, it can be concluded from the above discussion that individual ice crystals might have nucleated from individual jets but before 10 s of spray they fuse together and start proceeding as a single freezing front. Another conclusion that can be drawn through fig. 3.9 is the difference in the dimensions of ice ball formed due to the application of SHN and MHN; it is found to be 16 mm in lateral direction and 4 mm in axial direction. Spray zone formation and lower thermal conductivity of gel are the two responsible factors for such behavior. Spray zone is the area in which cryogen comes in direct contact with the gel surface. Larger spray zone of MHN is responsible for the growth of ice ball in lateral direction. Whereas, due to the lower thermal conductivity of gel, the ice ball propagation gets reduced in the axial direction. In the cryosurgery also, the propagation and shape of ice ball depend on the area of contact of cryoprobe with the tissue surface [54, 84, 130]. Due to this reason, ice ball formed has a semi-elliptic shape [159, 160].

### 3.2.3.3 Radial temperature distribution

Isometric view of tissue mimicking gel after 120 s of spray for various spraying distances of MHN is shown in fig. 3.10. An image of SHN is also included for comparison purpose (refer fig. 3.10d). The upper limit of the contour depicts the maximum temperature in the domain, i.e. temperature of human hand whereas the lower limit depicts  $-40^{\circ}\text{C}$  which is not the minimum temperature of the domain; the thermal imaging camera operates in the range of  $-40^{\circ}\text{C}$  to  $120^{\circ}\text{C}$ , so the minimum temperature it can capture is  $-40^{\circ}\text{C}$ . However, the actual temperature in those regions can be much lower than  $-40^{\circ}\text{C}$ .

**Movement of radial ice front**

Data extracted through fig. 3.10 is plotted with respect to the location on gel surface to estimate the extent of ice ball propagation as time progresses in fig. 3.11. Graph is plotted in such a way that 0 mm on abscissa represents the centre of spray. Maximum and minimum limits of abscissa demonstrate length of a diagonal on the gel surface. Ordinate represents temperature; it is not going below  $-40^{\circ}\text{C}$  due to the limitations of thermal imaging camera with respect to its temperature range. Two reference lines are also drawn along 0 mm on abscissa and  $0^{\circ}\text{C}$  on ordinate to enhance the understanding of graph. Image processing and data authentication method discussed in subsection 3.2.2 is followed to draw the curve. Fig. 3.11 depicts that the plot gets wider (with respect to  $0^{\circ}\text{C}$  reference line on ordinate) as the spray duration increases and the wideness of MHN is always greater than SHN. Here, wideness signifies the diameter of ice ball as graph is drawn with respect to CS which is symmetric about the axis. There is a constant difference of approximately 10 mm in diameter between the ice ball formed at  $0^{\circ}\text{C}$  by SHN and MHN, when  $z$  is kept constant at 18 mm. This difference remains same for the ice ball formed at lethal temperature, i.e.  $-40^{\circ}\text{C}$ . It signifies two important outcomes of the study: (i) the area of necrotic zone is larger in case of MHN as compared to SHN and (ii) difference in the diameter remains constant throughout the spray which means area of the necrotic zone can be easily manipulated while changing the duration of spray. Possible reason for this difference in diameter is the number of holes in MHN and the pattern of the holes. Symmetric nature of ice ball propagation is due to the pattern of holes, as they are inscribed in a circular pattern around the central hole.

Fig. 3.12 represents the movement of lethal front and freezing front on the surface of gel. The total spread of lethal front when  $z = 18$  mm is 32 mm and 21 mm for MHN and SHN respectively after 120 s of spray. While total spread of freezing front is found to be 46 mm and 30 mm for MHN and SHN respectively. The spread rate of lethal front with respect to time decreases as the time progresses because, diameter of lethal front is found to be 15 mm and 6 mm for MHN and SHN respectively after 30 s of spray. The steep gradient of spread rate during the initial stages of spray signifies the impact of spray zone formed due to the different nozzles. Spray zone of MHN would be larger than SHN due to the obvious reasons, which is responsible for a greater spread of lethal front in case of MHN.

Besides the comparison of SHN and MHN, the effect of spraying distance ( $z$ ) is considered through thermal images when MHN is used to spray cryogen. It has been observed that splashing of cryogen occurs after 60 s of spray when the spraying distance ( $z$ ) is 13 mm. The reason for such behavior is the reduction in the rate of evaporation of cryogen from its flight from nozzle exit to gel surface. Reduction in evaporation causes

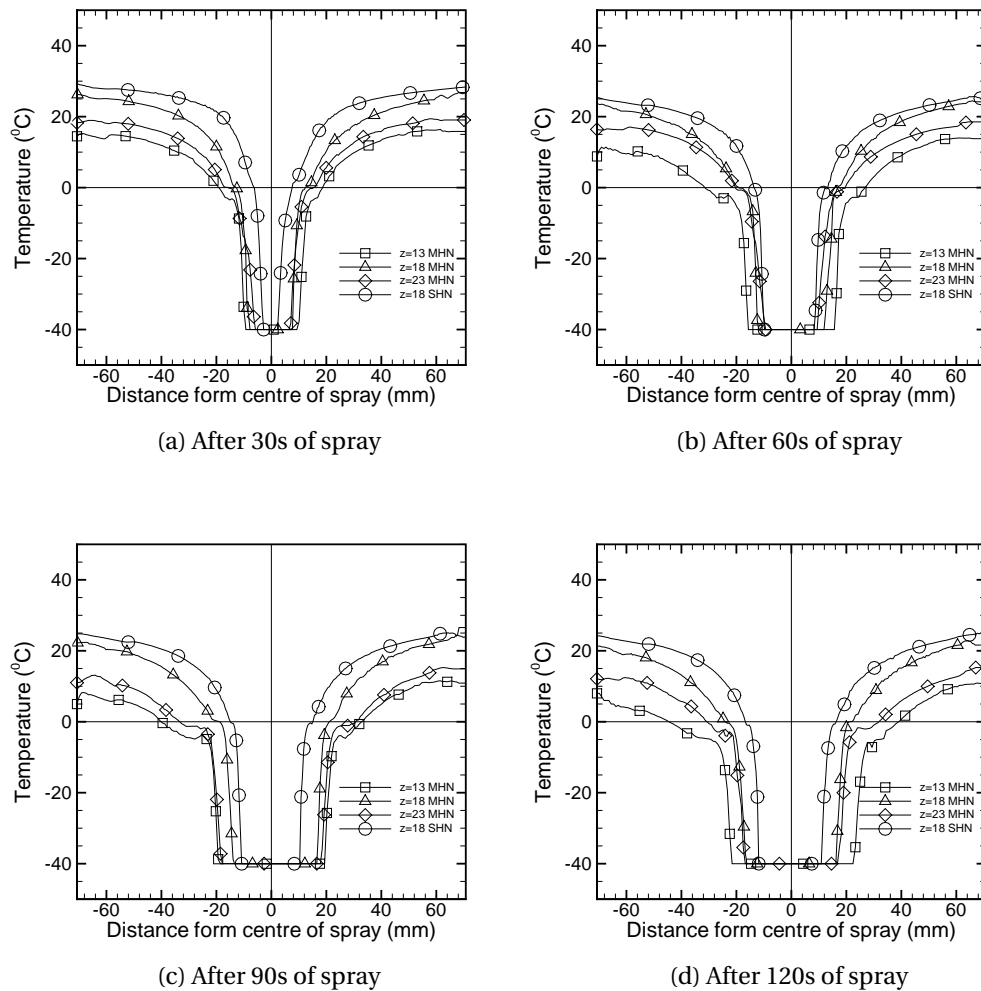


Figure 3.11: Temperature distribution along the gel surface (MHN: Multihole nozzle, SHN: Singlehole nozzle, z: Spraying distance)

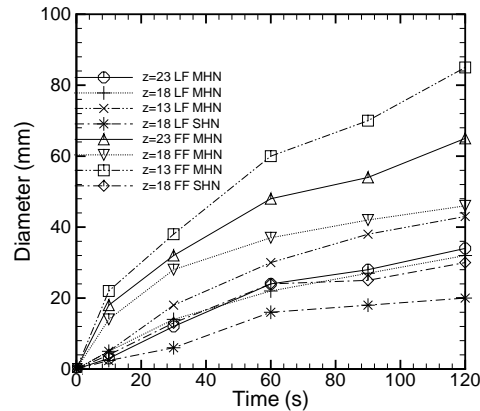


Figure 3.12: Movement of lethal and freezing front on gel surface (MHN: Multihole nozzle, SHN: Singlehole nozzle, z: Spraying distance, LF: Lethal front, FF: Freezing front)

larger droplet (in terms of diameter) to strike on the gel surface which causes splashing. Splashing is not observed in the initial stage of spray because the ice ball is not rigid during that stage. So the bouncing of cryogen is not observed during those stages. This behavior constrains the application of MHN with a spraying distance of  $z = 13$  mm because it can be detrimental for patient, especially if lesions occurring on face are treated. On the other hand, splashing is not observed when the spraying distance ( $z$ ) is 18 mm and 23 mm, which means all droplets get evaporated on the gel surface.

When spraying distance is changed for MHN, the temperature contour depicts an interesting phenomenon. For  $z = 18$  mm and 23 mm, the propagation of lethal front is almost identical but there is a huge difference in the propagation of freezing front. The difference between the freezing front and the lethal front is 14 mm and 30 mm when  $z = 18$  mm and 23 mm respectively. It means that with increase in the spraying distance small droplets envelop the gel surface which is responsible for larger ice ball formation. Since the droplets are smaller so the mass associated with them is also less which causes smaller lethal front formation even after having larger freezing front. This phenomenon constrains the use of  $z = 23$  mm in comparison to  $z = 18$  mm. For smallest spraying distance ( $z = 13$  mm) the difference in freezing front and lethal front is 40 mm which is also irrelevant as far as the feasibility of procedure is concerned. Also, the splashing problem associated with  $z = 13$  mm constrains its use in general practice. Hence,  $z = 18$  mm is the most optimised spraying distance.

### 3.2.4 Comparison among MHNs

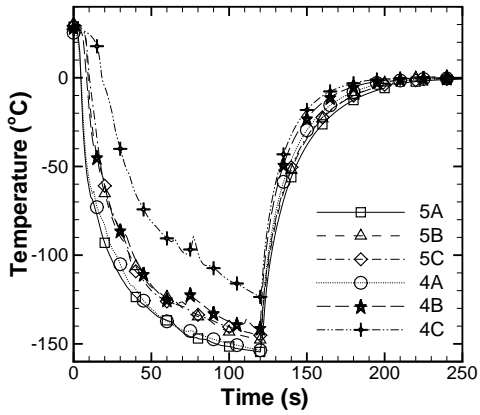
This section of the study presents a detailed discussion on the influence of various parameters of MHN on cryoablation. These parameters are number of hole, margin among the holes and the spraying distance. The most optimised spraying distance ( $z = 18$  mm) for MHN 5C is obtained through the aforementioned study (3.2.3). Thus, spraying distance of  $z = 18$  mm is chosen to spray the cryogen for all the MHNs (refer table. 3.1) used in the study. The influence of number of holes and margin among the holes is quantified on the basis of axial temperature distribution, radial temperature distribution and cooling rate obtained through the cryogen spray of different MHNs on tissue phantom.

#### 3.2.4.1 Axial temperature distribution

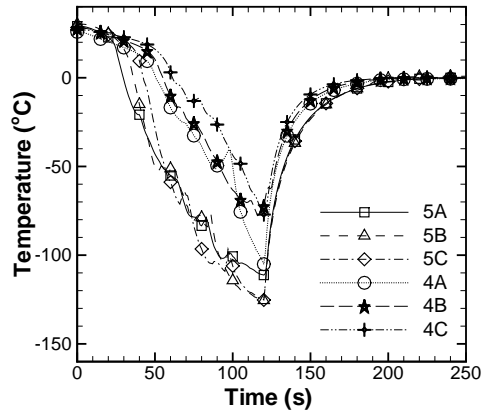
Fig. 3.13a represents temperature history for the thermocouple placed at TC200 location. MHNs with 5 holes register an end temperature of  $-154$  °C,  $-148$  °C and  $-145$  °C when margin among the hole is kept as 1 mm, 1.5 mm and 2 mm respectively after 120 s of spray. Similarly, MHNs with 4 holes (without central hole) register an end temperature of  $-153$  °C,  $-141$  °C and  $-123$  °C when margin among the hole is kept as 1 mm, 1.5 mm and 2 mm respectively after 120 s of spray. When the number of holes in MHNs are kept same, the end temperature increases with increase in the margin. The reason for such variation in end temperature can be attributed to the change in rate of evaporation of the cryogen when margin among the holes is changed. As the margin increases the distance between the jets of cryogen increases which allows more evaporation of cryogen. Thus, the less amount of cryogen reaches the gel surface in liquid form which ultimately reduces the extent of coldness.

However, if comparison between the number of holes in MHN is carried out keeping margin among the holes same. Slope of the curve and end temperature recorded by 5A and 4A are almost similar. Identical trend in slope is also recorded by 5B and 4B with slight variation in end temperature while 5C and 4C record variation in slope with appreciable difference in the end temperature. It reflects that although mass flow rate of cryogen changes when number of holes changes but at TC200 location influence of mass flow rate is less pronounced.

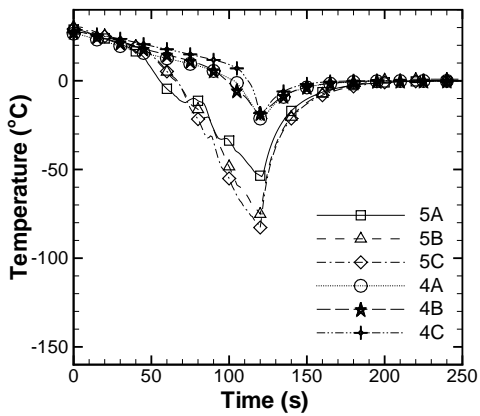
Furthermore,  $-111$  °C,  $-126$  °C and  $-125$  °C are the end temperature obtained through the thermocouple placed at TC210 location shown in fig.3.13b for MHNs 5A, 5B and 5C respectively while MHNs 4A, 4B and 4C provide end temperature of  $-105$  °C,  $-72$  °C and  $-77$  °C respectively for the same location. Unlike to TC200 location, if the comparison between the number of holes in MHN is carried out keeping margin among the holes same, it



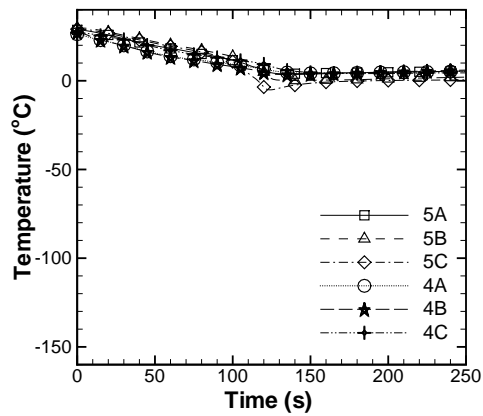
(a) 2 mm below gel surface and 0 mm away from CS



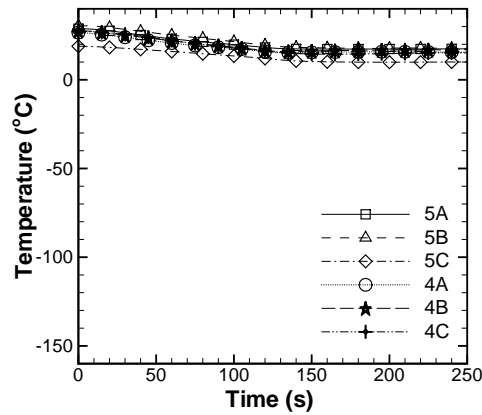
(b) 2 mm below gel surface and 10 mm away from CS



(c) 2 mm below gel surface and 15 mm away from CS



(d) 2 mm below gel surface and 20 mm away from CS

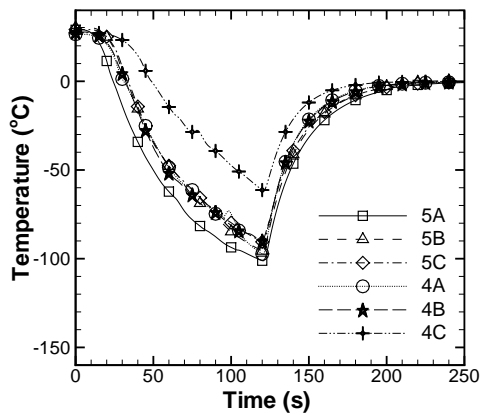


(e) 2 mm below gel surface and 25 mm away from CS

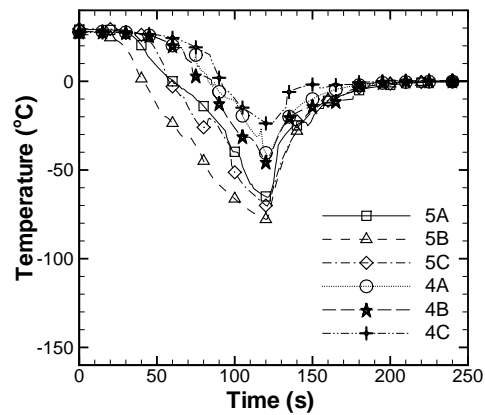
Figure 3.13: Transient temperature curves of thermocouples placed at 2 mm below the gel surface and at different radial locations

is interesting to note that both slope of the curve and end temperature show an appreciable difference. The influence of mass flow rate can be easily acknowledged at this location which is the main reason for variation in the slope of the curve and end temperature. Another significant variation that can be observed at this location is the temperature-time history of 5B and 5C. Lower end temperature as compared to 5A is recorded here in spite of the fact that at TC200 location, 5A registered the lowest temperature. Larger spray zone of 5B and 5C would be a possible reason for such variation. In contrast, 4B and 4C register higher end temperature as compared to 4A. This variation demarcates the role of the central hole, it causes less evaporation of cryogen as the distance between individual jets decreases due to it and larger spray zone formed due to increased margin provide more cryoablation in lateral direction. Similar curves of transient temperature are obtained for TC215 location as shown in fig. 3.13c. End temperature increases as the distance from the CS increases. Cooling below lethal temperature is not achieved in MHNs having 4 holes while MHNs with 5 holes are comfortably providing cooling below lethal temperature. As  $-53^{\circ}\text{C}$ ,  $-75^{\circ}\text{C}$  and  $-82^{\circ}\text{C}$  are the end temperature for 5A, 5B and 5C respectively while  $-21^{\circ}\text{C}$ ,  $-18^{\circ}\text{C}$  and  $-18^{\circ}\text{C}$  are the end temperature for 4A, 4B and 4C respectively. Thermocouples placed at the location TC220 and TC225 are less affected by the spray. It can be inferred that both margin among the holes and number of holes have a significant impact on cryoablation.

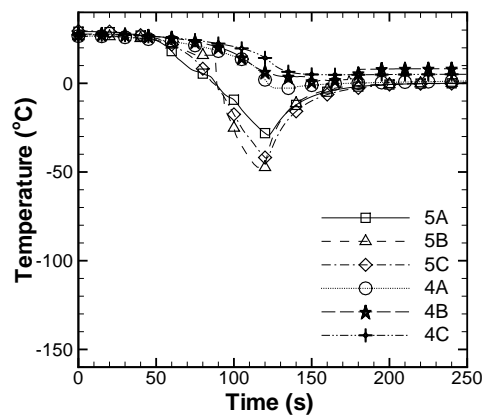
Variation of temperature with respect to time is shown in fig. 3.14a for TC500 location.  $-101^{\circ}\text{C}$ ,  $-95^{\circ}\text{C}$  and  $-90^{\circ}\text{C}$  are the end temperature recorded for MHNs 5A, 5B and 5C respectively whereas  $-97^{\circ}\text{C}$ ,  $-89^{\circ}\text{C}$  and  $-61^{\circ}\text{C}$  are the end temperature recorded for MHNs 4A, 4B and 4C respectively at TC500 location. It can be observed that at TC200 location approximately 80 % of end temperature is reached after 60 s of spray while at TC500 location only 50% of end temperature is achieved after 60 s of spray for all MHNs except 4C. It can be inferred from this observation, that as the distance from the CS increases the rate of heat transfer decreases due to lower thermal conductivity of gel. Thermal conductivity of gel remains constant with respect to temperature before freezing and it is inversely proportional to temperature during freezing [96, 164]. So, as the distance from CS increases the extent of freezing and temperature drop reduces which causes reduction in thermal conductivity of gel. This phenomenon ultimately decreases the rate of heat transfer. Similar observations can be found in the work of Kumari et al. [97]. They have conducted an experiment on the gel with SHN of diameter 0.8 mm from a spraying distance of 18 mm while mounting a thermocouple at the surface of gel. They achieved 90 % of end temperature within 20 s of spray. For TC510 location except 4C, cooling below lethal temperature is achieved in each nozzle. Compared to TC500 location, end temperature at this location



(a) 5 mm below gel surface and 0 mm away from CS



(b) 5 mm below gel surface and 10 mm away from CS



(c) 5 mm below gel surface and 15 mm away from CS

Figure 3.14: Transient temperature curves of thermocouples placed at 5 mm below the gel surface and at different radial locations

Table 3.4: CR ( $^{\circ}\text{C}/\text{min}$ ) for various thermocouples for various MHNs

MHN	Position of thermocouple							
	TC200	TC210	TC215	TC220	TC225	TC500	TC510	TC515
4A	76	52	10	-	-	48	20	-
4B	70	36	9	-	-	44	22	-
4C	61	38	9	-	-	30	11	-
5A	77	55	26	-	-	50	32	14
5B	73	62	37	-	-	47	38	23
5C	72	62	41	1	-	45	35	20

“-” Freezing of gel is not observed.

is higher which is expected because distance from CS increases.  $-64^{\circ}\text{C}$ ,  $-77^{\circ}\text{C}$ ,  $-70^{\circ}\text{C}$ ,  $-40^{\circ}\text{C}$ ,  $-45^{\circ}\text{C}$  and  $-23^{\circ}\text{C}$  are the end temperatures for MHNs 5A, 5B, 5C, 4A, 4B and 4C respectively as depicted in fig. 3.14b. From fig. 3.14c it is evident that temperature variation at TC515 location is following the same trend registered at TC510 location. Freezing of gel is not recorded when MHNs with 4 holes are implemented;  $4^{\circ}\text{C}$ ,  $6^{\circ}\text{C}$  and  $14^{\circ}\text{C}$  are end temperature of 4A, 4B and 4C respectively. Freezing of gel is observed in each case when MHNs with 5 holes are used; even cooling below lethal temperature is also recorded for 5B and 5C.  $-28^{\circ}\text{C}$ ,  $-47^{\circ}\text{C}$  and  $-41^{\circ}\text{C}$  are the end temperatures of 5A, 5B and 5C respectively.

All these temperature measurements have a commonality; temperature suddenly rises from end temperature to  $0^{\circ}\text{C}$  as the freezing cycle ends and increases gradually with further thaw duration. Huge temperature difference between the ice ball (formed due to cryogen spray) and the gel would be a possible reason for such behavior.

Thus, it can be concluded from above discussions that central hole plays an important role in cryoablation because it reduces the rate of evaporation of cryogen while increasing its mass flow rate. Among the MHNs with 5 holes, 5B is providing the maximum cryoablation. The reason can be attributed to 1.5 mm margin between the holes, which increases the spray zone of cryogen when compared to 5A and reduces the rate of evaporation when compared to 5C.

### 3.2.4.2 Cooling rate

Table 3.4 lists the cooling rate at discrete locations for different MHNs. The data mentioned in table 3.4 reflects clearly that MHNs with 5 holes are providing higher cooling rate than MHNs with 4 holes at same location. Intracellular ice formation is observed at TC200 location for all MHNs. For TC210 location MHNs with 5 holes are achieving cooling rate higher than  $50^{\circ}\text{C}/\text{min}$  while only 4A is crossing the threshold of intracellular ice formation when the MHNs with 4 holes are considered. At TC215 location, influence of reduced mass

Table 3.5: Movement of lethal front and freezing front (in mm) on the gel surface with respect to time

Time (s)	4A		4B		4C		5A		5B		5C		SHN	
	LF	FF	LF	FF	LF	FF	LF	FF	LF	FF	LF	FF	LF	FF
30	16	27	11	25	10	20	18	28	14	24	14	28	6	13
60	22	34	20	33	18	32	26	36	22	36	22	37	16	24
90	26	40	26	38	24	39	30	42	26	46	27	42	18	26
120	32	46	30	45	28	42	34	50	30	50	32	46	20	30

LF: Temperature less than  $-40^{\circ}\text{C}$   
FF: Temperature less than  $-40^{\circ}\text{C}$

flow rate and increment in rate of evaporation due to absence of central hole is responsible for lower cooling rates of 4A, 4B and 4C. Cooling below lethal temperature ensures the criteria of 100 % cryoablation for MHNs with 5 holes. At TC220 and TC225 freezing of gel is not observed which means necrotic zone is limited to 30 mm across the gel surface at an axial depth of 2 mm from surface for MHNs with 5 holes. For MHNs with 4 holes it would be smaller than the former case because 100% cell destruction cannot be assured at TC215 location due to lower cooling rate and end temperature. At an axial depth of 5 mm below the CS, i.e. TC500 location, necrosis of tissue can be assured due to combination of intracellular and extracellular ice formation. Although intracellular ice formation would be more than extracellular ice formation at this location, because CR ranges in between  $30\text{-}50^{\circ}\text{C}/\text{min}$  [73, 87]. Similarly at TC510 all MHNs except 4C are providing 100% cryoablation even after having lower cooling rate because cooling below lethal temperature is achieved in all the cases. Influence of reduced mass flow rate of cryogen can be noticed at TC515 location, where freezing is not observed when MHNs with 4 holes are employed. Although necrosis can be assured with MHNs with 5 holes at the same location [41]. It can be interpreted through the data of end temperature and cooling rate that the necrotic zone would approximate an elliptic shape, similar to shape of the ice ball [96, 97]. The dimensions of semi-major and semi-minor axes should be in between 15-20 mm and 5-8 mm respectively for MHNs with 5 holes while for MHNs with 4 holes it would be in between 10-15 mm for semi-major axis and 5-8 mm for semi-minor axis.

### 3.2.4.3 Radial temperature distribution

The data extracted through temperature contours [133] of thermal images are mentioned in table 3.5. Rate of lethal front and ice front propagation for each nozzle decreases as the time progress. Spray zone formation and lower thermal conductivity of gel are the two responsible factors for such behavior. Spray zone is the area in which cryogen comes in

direct contact with the gel surface. Larger spray zone of MHNs are responsible for initial growth of ice ball. Whereas, due to lower thermal conductivity of gel as the time progresses the propagation of ice ball gets reduced. Similar behavior of ice ball propagation can be observed in the work of Kumari et al. [97]. In cryosurgery as well propagation and shape of ice ball depends on area of contact of cryoprobe and tissue surface [54, 76, 84, 130]. Symmetric nature of ice ball propagation is observed in each nozzle. It is due to the pattern of holes as they are inscribed in a circular pattern around the central hole due to which multiple freezing fronts produced by individual jet of MHN get clubbed together to form a giant ice ball.

Data of table 3.5 advocates that as the margin increases the diameter of lethal front decreases if number of holes in the MHNs are kept constant. Increase in margin causes increase in the rate of evaporation of cryogen accompanied with formation larger spray zone. Larger spray zone aids in the formation larger ice ball but rapid evaporation reduces the diameter of droplets reaching the gel surface. Smaller droplets causes reduction in the extent of coldness on gel surface which leads to smaller ice ball formation. Thus, it can be interpreted from the entries of table 3.5 that effect larger spray zone is less dominant than the rate of evaporation in the formation ice ball. Lethal front MHNs with 5 holes is larger than MHNs with 4 holes for same margin. Higher mass flow rate is responsible for formation larger spray zone in MHNs with 5 holes.

#### **3.2.4.4 Conclusion**

Present study proposes a unique idea of increasing efficacy of cryospray process through the application of MHN. A prototype of MHN is manufactured and tested under similar conditions that are followed in current practice. To ensure the authenticity of results a comparative study is carried out between the customised and commercial nozzle for the same spraying distance. Furthermore, most optimised spraying distance for maximum cryoablation is also determined when MHN is used to spray cryogen. Furthermore, after the establishment of most optimised spraying distance comparative study among the six MHNs are carried out for same spraying distance. Following conclusions can be drawn through present study:

- More uniform and larger spread of cryogen through application of MHN can reduce the inability of existing cryospray process to treat larger lesions. Due to smaller spray zone of SHN, surgeons have to opt overlapping technique for the treatment of larger lesion. In this technique, surface area of lesion is divided into several parts. Selective freezing is carried out on that limited part of lesion and it continues until the whole lesion is covered. It increases the duration of treatment.

- The ratio of lateral spread to axial depth of the ice ball is found to be 3 for SHN while it is found to be 3.3 for MHN, for the same spraying distance of  $z = 18$  mm after 120 s of spray. It reflects that even after having multiple holes, ratio of lateral spread to axial depth of ice ball for MHN is almost same as SHN.
- The most optimised spraying distance for MHN is found to be 18 mm. It is also noted that the difference between lethal front and freezing front remains constant throughout the process with  $z = 18$  mm. It will help in assigning margin along the lesion.
- Central hole plays a crucial role in increasing the cryoablation. Central hole not only increases the mass flow rate but also reduces the evaporation of cryogen ejecting from individual jets of MHNs.
- 1.5 mm margin provides the most promising result among the 3 margins selected for the study, when nozzles with central hole are considered. For nozzles without central hole, 1 mm margin provides the maximum cryoablation.